Roll Resonance Control of Angle of Attack for Reentry Vehicle Drag Modulation

Prepared by
D. H. PLATUS
Aerophysics Laboratory
Laboratory Operations
The Aerospace Corporation
El Segundo, Calif. 90245

10 December 1980

Interim Report

Prepared for

SPACE DIVISION
AIR FORCE SYSTEMS COMMAND
Los Angeles Air Force Station
P.O. Box 92960, Worldway Postal Center
Los Angeles, Calif. 90009

This interim report was submitted by The Aerospace Corporation, El Segundo, CA 90245, under Contract No. F04701-79-C-0080 with the Space Division, P.O. Box 92960, Worldway Postal Center, Los Angeles, CA 90009. It was reviewed and approved for The Aerospace Corporation by W. R. Warren, Jr., Director, Aerophysics Laboratory. Lieutenant James C. Garcia, SD/YLVS, was the project officer for Mission-Oriented Investigation and Experimentation (MOIE) Programs.

This report has been reviewed by the Public Affairs Office (PAS) and is releasable to the National Technical Information Service (NTIS). At NTIS, it will be available to the general public, including foreign nations.

This technical report has been reviewed and is approved for publication. Publication of this report does not constitute Air Force approval of the report's findings or conclusions. It is published only for the exchange and stimulation of ideas.

James C. Garcia

J. C. Garcia, Lt, USAF
Project Officer

Kenneth E. Needham

Kenneth E. Needham, LtCol, USAF
Chief, Space Vehicle Subsystems Division

FOR THE COMMANDER

Florian P. Meinhardt

Florian P. Meinhardt, LtCol, USAF
Director, Directorate of Advanced Space Development
Deputy for Technology

UNCLASSIFIED

SECURITY CLASSIFICATION OF THIS PAGE (When Data Entered)

REPORT DOCUMENTATION PAGE

READ INSTRUCTIONS BEFORE COMPLETING FORM

1. REPORT NUMBER: SD-TR-80-84	2. GOVT ACCESSION NO.: AD-A093741
3. RECIPIENT'S CATALOG NUMBER:	
4. TITLE (and Subtitle): ROLL RESONANCE CONTROL OF ANGLE OF ATTACK FOR REENTRY VEHICLE DRAG MODULATION	5. TYPE OF REPORT & PERIOD COVERED: Interim rept.
	6. PERFORMING ORG. REPORT NUMBER: TR-0081(6940-02)-4
7. AUTHOR(s): D. H. Platus	8. CONTRACT OR GRANT NUMBER(s): F04701-80-C-0081
9. PERFORMING ORGANIZATION NAME AND ADDRESS: The Aerospace Corporation, El Segundo, Calif. 90245	10. PROGRAM ELEMENT, PROJECT, TASK AREA & WORK UNIT NUMBERS: F04701-79-C-0080
11. CONTROLLING OFFICE NAME AND ADDRESS: Space Division, Air Force Systems Command, Los Angeles, Calif. 90009	12. REPORT DATE: 10 Dec 1980
	13. NUMBER OF PAGES: 24
14. MONITORING AGENCY NAME & ADDRESS (if different from Controlling Office): 12 29	15. SECURITY CLASS. (of this report): Unclassified
	15a. DECLASSIFICATION/DOWNGRADING SCHEDULE

16. DISTRIBUTION STATEMENT (of this Report)

Approved for public release; distribution unlimited

17. DISTRIBUTION STATEMENT (of the abstract entered in Block 20, if different from Report)

18. SUPPLEMENTARY NOTES

19. KEY WORDS (Continue on reverse side if necessary and identify by block number)

Drag Control
Drag Modulation
Reentry Aerodynamics
Reentry Control
Reentry Dynamics
Reentry Vehicle Drag Control
Reentry Vehicle Recovery

20. ABSTRACT (Continue on reverse side if necessary and identify by block number)

Slender ballistic reentry vehicles are highly susceptible to roll rate changes caused by small asymmetries in mass and configuration. One particular combination of asymmetries, consisting of a body-fixed trim angle of attack and a small radial c.g. offset, can cause a rapid spinup into resonance, with a large amplification in trim angle of attack and a concomitant increase in drag. By controlling the magnitude and direction of the c.g. offset with a moving-mass roll control system, it is possible to control the roll rate near resonance and to -

DD FORM 1473 (FACSIMILE)

409367

UNCLASSIFIED

SECURITY CLASSIFICATION OF THIS PAGE (When Data Entered)

19. KEY WORDS (Continued)

20. ABSTRACT (Continued)

limit the angle-of-attack and drag response to a controlled value. A feedback law is derived, and the control system is demonstrated with a digital-computer simulation of the equations of rotational motion.

CONTENTS

I. INTRODUCTION..... 5

II. CONTROL ANALYSIS..... 7

III. APPLICATION TO RECOVERY..... 15

IV. NUMERICAL EXAMPLE..... 17

V. CONCLUSIONS..... 25

REFERENCES..... 27

GLOSSARY..... 29

FIGURES

1. Asymmetries and roll orientation..... 8

2. Superresonant condition..... 10

3. Root loci..... 13

4. Idealized approximation to C_{m_q} 19

5. Roll-rate response, c.g. offset movement, and windward-meridian angle..... 21

6. Response to 400 g acceleration command..... 22

7. Recovery angle of attack and velocity..... 23

I. INTRODUCTION

It is well known that a slender, high-performance ballistic reentry vehicle is susceptible to roll resonance caused by small asymmetries in mass and configuration.[1-4] The vehicle can exhibit large roll-rate excursions because of its low roll moment of inertia and the extreme aerodynamic pressures during atmospheric entry. The vehicle is most susceptible to a body-fixed trim asymmetry with an orthogonal component of radial c.g. offset. Lift caused by the trim angle of attack acts on the c.g. offset moment arm to produce a roll torque that can spin the vehicle rapidly into resonance. A trim-angle-of-attack asymmetry on the order of 1 deg or less in conjunction with a radial c.g. offset on the order of tens of thousandths of an inch can cause large roll rate excursions sufficient to spin the vehicle into resonance. The trim angle of attack can be amplified in resonance by a factor of 10 to 15 or more, depending on the altitude at which resonance is encountered. As a preventive measure, vehicles must be accurately balanced to minimize radial displacement of the center of gravity from the aerodynamic axis of symmetry. In some cases, roll control is also required.

Described here is a method of utilizing roll resonance in a controlled manner for drag modulation. Large angle-of-attack-induced drag can be used to decelerate a test vehicle for recovery,[5] or drag modulation can be used to compensate for drag uncertainty in order to control range errors.[6] The control system consists of a moving-mass roll control, strapdown motion sensors, and a built-in trim-angle-of-attack asymmetry. During roll resonance, the roll rate is approximately equal to the undamped natural pitch frequency, which can become quite large for a ballistic reentry vehicle near peak dynamic pressure. However, the frequency at which the roll rate oscillates about the critical frequency, which determines the response frequency of the moving-mass control system, is considerably lower than the pitch frequency. This feature of the control system as well as the relatively small mass required for c.g. control greatly simplifies the practical implementation of the system. A feedback law is derived from a linear approximation to the

moment equations of motion near resonance. The control system as applied to recovery is demonstrated with a digital-computer simulation of the nonlinear moment equations of motion.

II. CONTROL ANALYSIS

The small-angle equations of rotational motion in terms of classical Euler angles or wind-referenced coordinates can be written

$$\ddot{\theta} + (\omega^2 - \dot{\psi}^2)\theta + \nu\dot{\theta} = \omega^2\tau \cos(\phi + \phi_0) \tag{1}$$

$$\frac{d}{dt}(\dot{\psi}\theta) + \ddot{\theta}\psi + \nu\dot{\psi}\theta = \omega^2\tau \sin(\phi + \phi_0) \tag{2}$$

$$\dot{p} = -\eta\theta c \sin\phi \tag{3}$$

in which τ is a body-fixed, nonrolling trim angle of attack oriented at an angle ϕ_0 with respect the plane of a radial c.g. offset c (Fig. 1). The roll angle ϕ is a measure of the orientation of the plane of c.g. offset with respect to the wind plane. We will consider the case in which the trim is orthogonal to the plane of c.g. offset ($\phi_0 = 90$ deg), which will cause a rapid spinup into resonance. We assume, *a priori*, the quasi-steady condition

$$\dot{\psi} \approx \omega = \text{const} \tag{4}$$

which, with the small-angle definition of p

$$p = \dot{\phi} + \dot{\psi} \tag{5}$$

gives, for Eqs. (2) and (3),

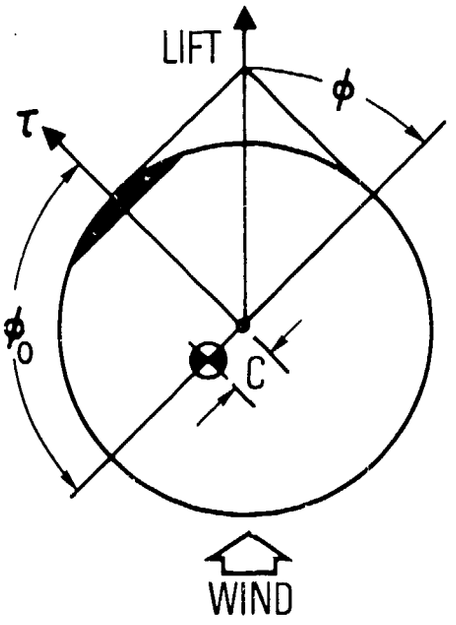

Fig. 1 Asymmetries and roll orientation

$$\dot{\theta} + \frac{\nu}{2}\theta = \frac{\omega\tau}{2}\cos\phi \tag{6}$$

$$\ddot{\phi} + \eta\theta c \sin\phi = 0 \tag{7}$$

We further assume that the vehicle spins through resonance so that the body-fixed trim plane is oriented nominally 180 deg from its nonrolling orientation, $\phi = -90$ deg (Fig. 2), and define a new roll angle ε

$$\varepsilon = \frac{\pi}{2} - \phi \tag{8}$$

If we assume that ε is a small angle, Eqs. (6) and (7) can be written

$$\dot{\theta} + \frac{\nu}{2}\theta = \frac{\omega\tau}{2}\varepsilon \tag{9}$$

$$\ddot{\varepsilon} - \eta\theta c = 0 \tag{10}$$

As the vehicle spins into resonance, the moving-mass controller will adjust the center of gravity offset to cause a roll response that will control the angle of attack or normal acceleration according to some control law. We select a control law

$$c = -\frac{K_1\dot{\varepsilon} + K_2(\theta - \theta_c) + K_3\dot{\theta}}{\eta\theta} \tag{11}$$

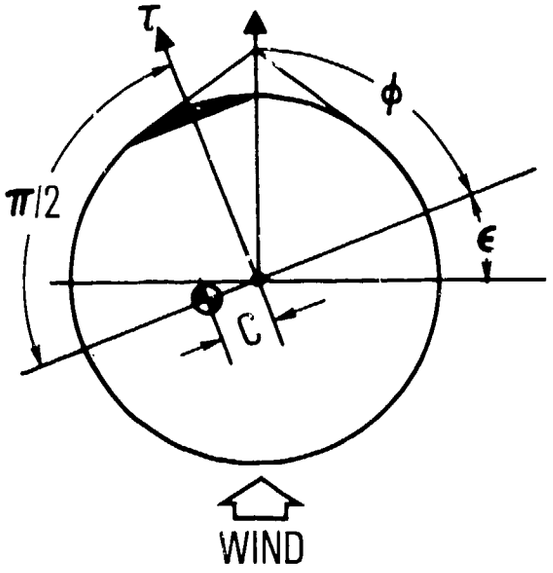

Fig. 2. Superresonant condition

in which θ_c is a command value of angle of attack (or normal acceleration). Equation (11) substituted in Eq. (10) gives

$$\ddot{\varepsilon} + K_1\dot{\varepsilon} + K_2(\theta - \theta_c) + K_3\dot{\theta} = 0 \tag{12}$$

which, with Eq. (9), yields two coupled control equations in θ and ε. We can solve for θ from Eqs. (9) and (12) by the use of Laplace transforms, which gives

$$\left[s^3 + \left(K_1 + \frac{\nu}{2}\right)s^2 + \left(\frac{\nu}{2}K_1 + \frac{\omega\tau}{2}K_3\right)s + \frac{\omega\tau}{2}K_2\right]\theta(s) = \frac{\omega\tau}{2}K_2\theta_c(s) \tag{13}$$

Consider the response to a step command $\theta_c(t) = \theta_c$. Equation (13) can then be written

$$\theta(s) = \frac{K\theta_c}{s(s + a)\ (s + b)\ (s + c)} \tag{14}$$

where

$$(s + a)(s + b)(s + c) = s^3 + \left(K_1 + \frac{\nu}{2}\right)s^2 + \left(\frac{\nu}{2}K_1 + \frac{\omega\tau}{2}K_3\right)s + K \tag{15}$$

and $K = \omega\tau K_2/2$. We can obtain a, b, and c from a root locus in which the transfer function G is

$$G = \frac{K}{s\left[s^2 + \left(K_1 + \frac{\nu}{2}\right)s + \frac{\nu}{2} K_1 + \frac{\omega\tau}{2} K_3\right]} \tag{16}$$

Two possible root loci are shown in Fig. 3, depending on the coefficients of s in Eq. (16). For a stable solution, either three negative real roots or one negative real and two complex conjugate roots are possible. The inverse Laplace transform of Eq. (14) yields the time response to the step command θ_c

$$\begin{aligned} \frac{\theta(t)}{K\theta_c} = \frac{1}{abc} &- \frac{1}{a(a-b)(a-c)} e^{-at} \\ &- \frac{1}{b(b-a)(b-c)} e^{-bt} \\ &- \frac{1}{c(c-a)(c-b)} e^{-ct} \end{aligned} \tag{17}$$

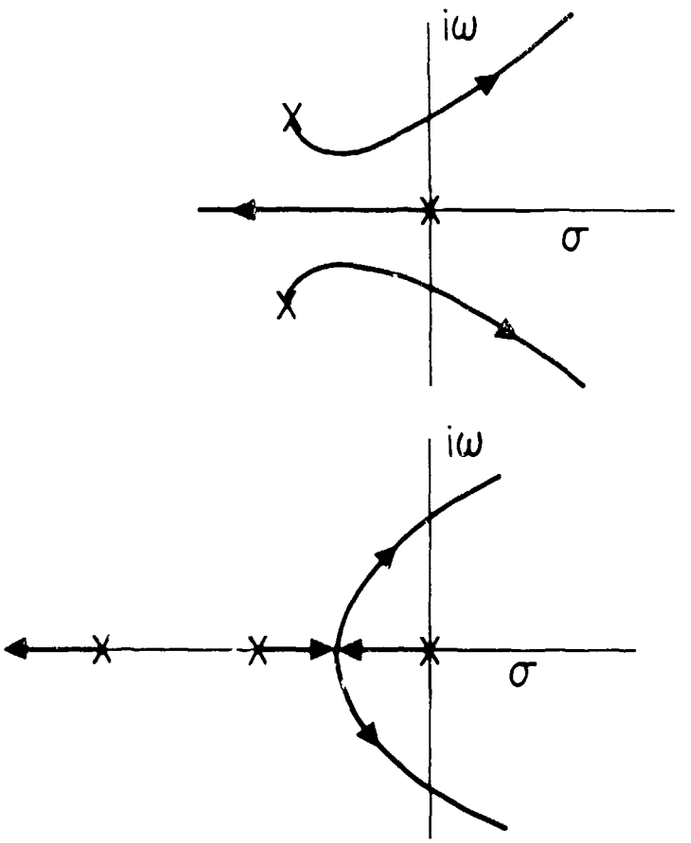

Fig. 3. Root loci

III. APPLICATION TO RECOVERY

The large-angle pitch and yaw equations equivalent to Eqs. (1) and (2) can be written[5]

$$\ddot{\theta} - \dot{\psi}^2 \sin\theta \cos\theta + \nu\dot{\theta} = \omega^2\tau \cos(\phi + \phi_0) - \frac{C_N(\theta)\, qSx_{st}}{I} \tag{18}$$

$$\frac{d}{dt}(\dot{\psi} \sin\theta) + \dot{\theta}\dot{\psi} \cos\theta - \mu p\dot{\theta} + C^*_{m_q} \dot{\psi} \sin\theta - C^*_{N_\alpha} \mu p\theta = \omega^2\tau \sin(\phi + \phi_0) + \frac{C^*_{N_\alpha} C_L(\theta)\, \dot{\psi} \sin\theta \cos\theta}{C_N(\theta)} \tag{19}$$

in which the lift coefficient $C_L(\theta)$ and the normal force coefficient $C_N(\theta)$ can be approximated by the sharp cone Newtonian relations.[7] For $\theta < \sigma$

$$C_N(\theta) = \cos^2\sigma \sin 2\theta \tag{20}$$

$$C_A(\theta) = 2 \sin^2\sigma + (1 - 3 \sin^2\sigma) \sin^2\theta \tag{21}$$

and for $\theta > \sigma$

$$C_N(\theta) = (\cos^2\sigma \sin 2\theta)\left[\left(\frac{\beta + \pi/2}{\pi}\right) + \left(\frac{\cos\beta}{3\pi}\right)\left(\lambda + \frac{2}{\lambda}\right)\right] \tag{22}$$

$$C_A(\theta) = \left(\frac{\beta + \pi/2}{\pi}\right)\left[2\sin^2\sigma + \left(1 - 3\sin^2\sigma\right)\right] + \frac{3}{4\pi}\cos\beta \sin 2\theta \sin 2\sigma \tag{23}$$

where σ = cone half-angle, $\lambda \equiv \tan\sigma/\tan\theta$, $\beta \equiv \sin^{-1}\lambda$, and

$$C_D(\theta) = C_A(\theta)\cos\theta + C_N(\theta)\sin\theta \tag{24}$$

$$C_L(\theta) = C_N(\theta)\cos\theta - C_A(\theta)\sin\theta \tag{25}$$

We can estimate influence of the angle of attack and drag on the trajectory from Eqs. (3), (18) and (19) in conjunction with the trajectory equations[5]

$$\frac{du}{dt} = -\frac{C_D qS}{m} + g\sin\gamma \tag{26}$$

$$\frac{dh}{dt} = -u\sin\gamma \tag{27}$$

$$\frac{d\gamma}{dt} = \left(\frac{g}{u} - \frac{u}{R_E + h}\right)\cos\gamma \tag{28}$$

The moving-mass controller is simulated by the c.g. offset relation given in Eq. (11) in which $\dot{\epsilon} = -\dot{\phi}$ according to Eq. (8). The function of the control system is to limit the normal acceleration to some acceptable value, while providing sufficient angle-of-attack-induced drag to decelerate the vehicle from hypersonic velocity at recovery-initiation altitude to a soft landing.

IV. NUMERICAL EXAMPLE

The equations of motion were solved numerically for a recovery simulation in which a ballistic reentry vehicle is spun into resonance at an altitude of 15 kft. The moving-mass controller is utilized to control the growth of angle of attack in order to limit the normal acceleration to a prescribed maximum value. The angle of attack is related to normal acceleration A_N according to

$$C_N(\theta) = \frac{mg\ A_N}{qS} \tag{29}$$

which, for small angles, can be written

$$\theta = \frac{mg}{C_{N_\alpha} qS}\ A_N = \frac{mg\ x_{st}}{\omega^2 I}\ A_N \tag{30}$$

The control law Eq. (11), expressed in terms of normal acceleration and normal acceleration command A_{N_C} is

$$c = \frac{1}{\eta_1 \sin\phi}\left[K_1\dot{\phi} + K_2 \frac{mg\ x_{st}}{\omega^2 I}\left(A_{N_c} - A_N\right) - K_3\dot{\theta}\right] \tag{31}$$

The control configuration is such that the plane of c.g. control is orthogonal to the plane of trim asymmetry (ϕ_0 = 90 deg in Fig. 1). The vehicle having the aerodynamic and mass properties listed below is subjected to a suddenly applied trim-angle-of-attack asymmetry τ = 1.5 deg with an initial c.g. offset of 0.050 in.

$C_{m_q} = -6$

$C_{N_\alpha} = 2$

$d = 0.958$ ft

$I = 3.70$ slug-ft^2

$I_x = 0.140$ slug-ft^2

$m = 3.79$ slugs

$S = 0.721$ ft^2

$x_{st} = 0.468$ ft

$h_o = 15$ kft

$U_o = 15.75$ kft/sec

$\gamma_o = 26$ deg

$\sigma = 6$ deg

$p_o = 50$ rad/sec

$A_{N_C} = 400$ g

As the vehicle spins into resonance, the c.g. offset is controlled according to Eq. (31), in which the feedback gains are as follows:

$t \leq 1.33$ sec: $K_1 = 54$, $K_2 = 22469$, $K_3 = 400$

$t > 1.33$ sec: $K_1 = 31.6$, $K_2 = 845$, $K_3 = 200$

The gains were estimated from the linear results of Eqs. (14) through (16) to give a stable solution and were changed once to accommodate the large change in dynamic pressure and vehicle characteristic frequencies as the vehicle decelerates. The large angle-of-attack aerodynamics are calculated from the Newtonian approximations, Eqs. (20) through (25), and the pitch damping derivative, C_{m_q}, is altered as a function of angle of attack, as shown in Fig. 4, to approximate the destabilizing effects of vortex shedding at large incidence described in NASA Ames experiments.[8,9]

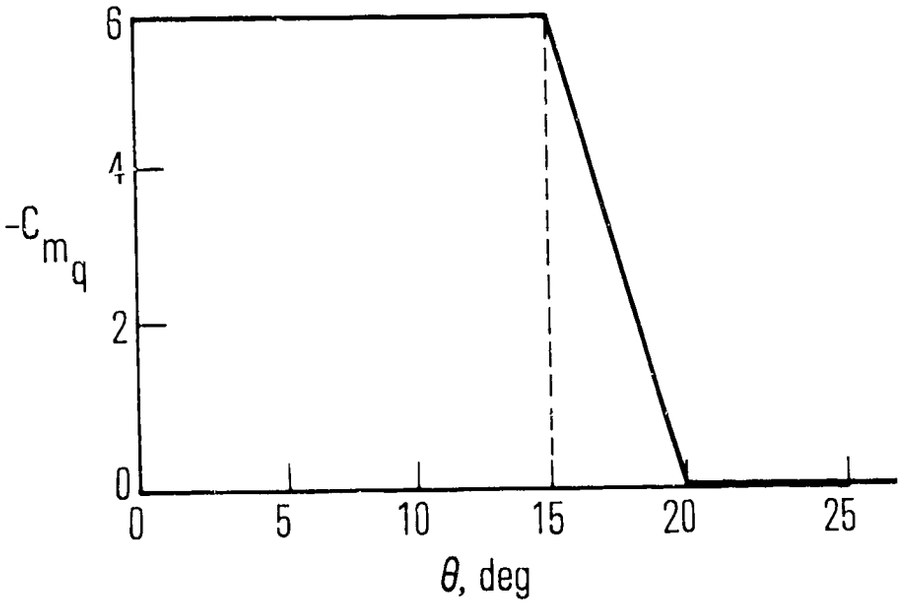

Fig. 4. Idealized approximation to C_{m_q}

Results of the computer simulation are shown in Figs. 5 through 7. The roll rate response relative to the critical roll rate is shown in Fig. 5a, the c.g. offset movement is shown in Fig. 5b, and the windward-meridian angle ϕ is shown in Fig. 5c. The normal acceleration response to the command value of 400 g is shown in Fig. 6, and the angle of attack and velocity behavior are shown in Fig. 7. The angle-of-attack growth in resonance with the body-fixed trim asymmetry drives the vehicle into a flat spin at 90-deg angle of attack. A significant feature of the control system response is the relatively low frequency of the c.g. offset or moving-mass oscillations compared with the characteristic pitch frequency of the vehicle. This can be seen from Eq. (7) for the linear approximation to the roll angle oscillations relative to the wind. For small oscillations in ϕ, Eq. (7) represents a harmonic oscillator with natural frequency Ω given by

$$\Omega = (\eta\theta c)^{1/2} \approx \omega\left[\left(\frac{c}{x_{st}}\right)\left(\frac{I}{I_x}\right)\theta\right]^{1/2} \tag{32}$$

In the time period around 0.5 to 1 sec, from Figs. 5 and 7, $c \approx 0.015$ in., $\theta \approx 12$ deg and $\omega \approx 25$ cps, which gives for Ω the value $0.12\,\omega$ or 3 cps. This agrees well with the oscillation frequency observed in Fig. 5. The c.g. offset amplitude required for control is approximately $\pm$ 0.020 in., from Fig. 5b. This requires a moving-mass throw weight of only 2.5 lb-in., e.g., a 2.5-lb mass with a displacement of $\pm$1 in. or a 1.25-lb mass with a displacement of $\pm$2 in., for the 122-lb example vehicle. In view of the relatively low oscillation frequency required for this mass, the energy requirements of the controller are minimal.

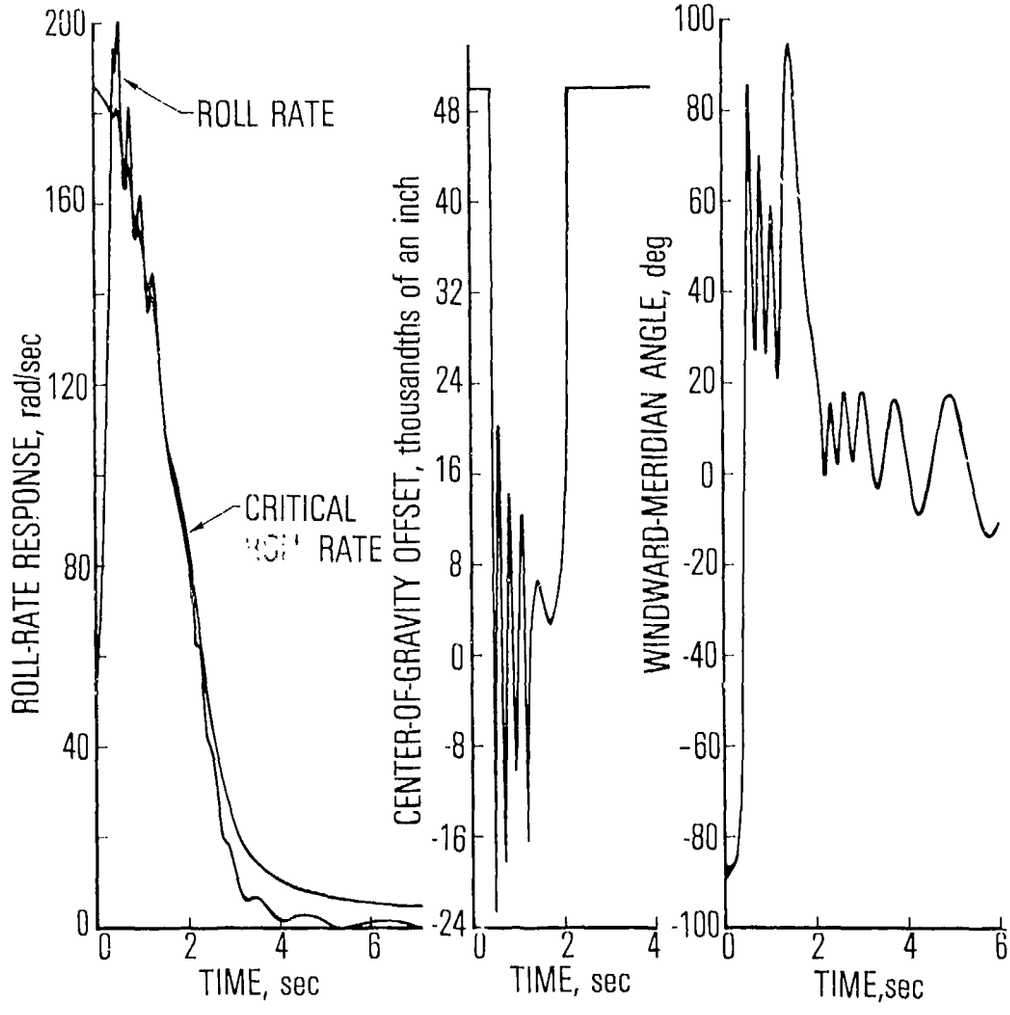

Fig. 5. Roll-rate response, c.g. offset movement, and windward-meridian angle

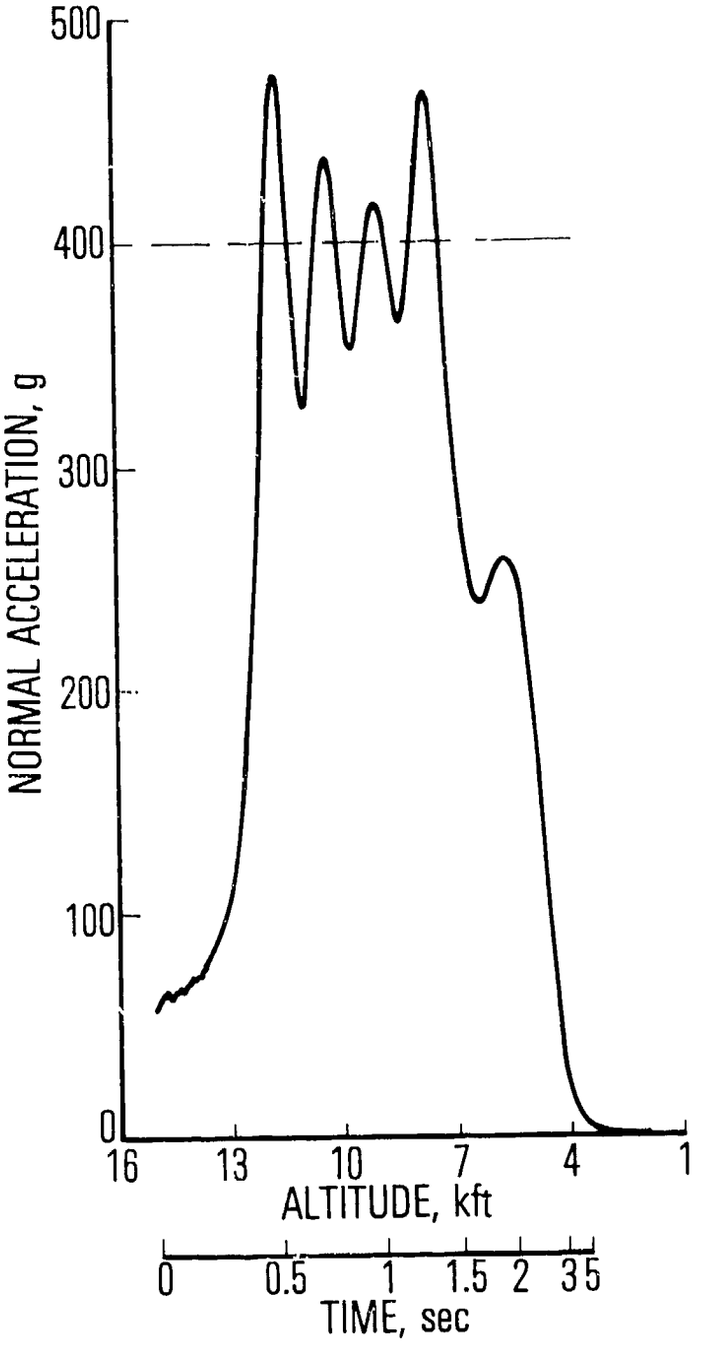

Fig. 6. Response to 400-g acceleration command

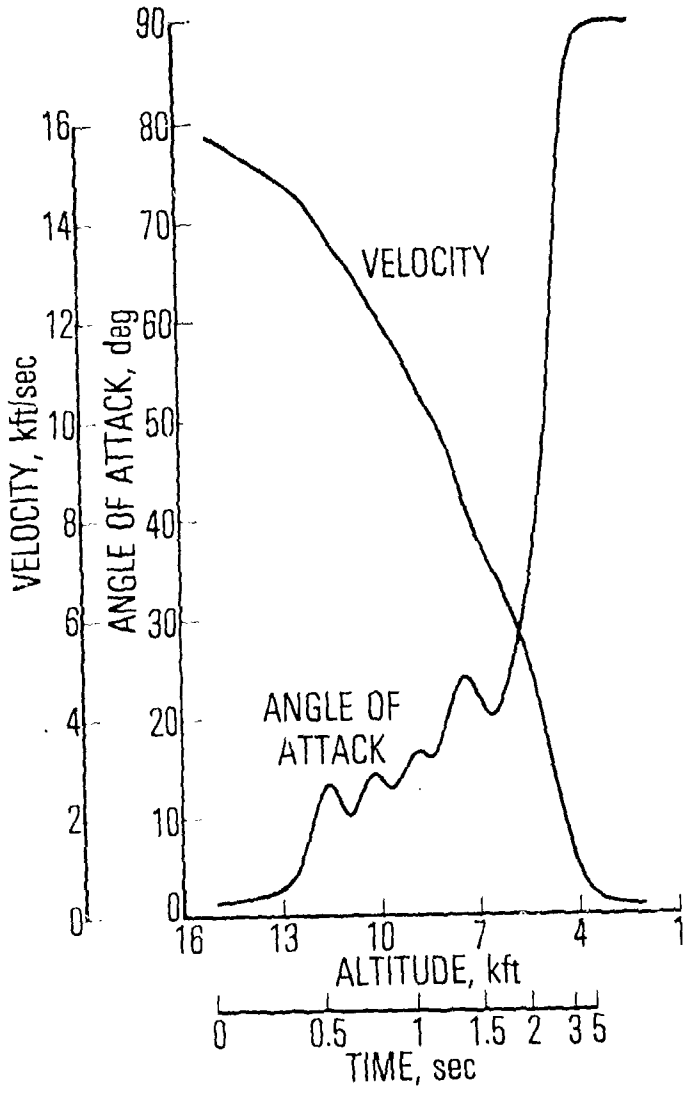

Fig. 7. Recovery angle of attack and velocity

V. CONCLUSIONS

The concept of using a moving-mass center-of-gravity controller to limit roll resonance angle-of-attack amplification of a ballistic reentry vehicle has been demonstrated. A control law derived from a first-order linear approximation to the nonlinear rotational equations of motion near resonance yields a stable response to an angle-of-attack control system. The first order solution, obtained with little optimization, is an indication of the stability of the resonance lockin condition driven by a body-fixed trim asymmetry with an orthogonal center-of-gravity offset. A significant feature of the resonant motion is the relatively low frequency of coupled oscillations in angle of attack, roll rate, and roll angle, about the steady-resonance condition. This low-frequency motion determines the response requirements of a moving-mass c.g. controller, and the energy requirements prove to be minimal. The resonance control system has been demonstrated with an application to ballistic reentry vehicle recovery. The controller can limit the angle of attack and normal load response in resonance, while providing a large angle-of-attack-induced drag for recovery. A digital-computer simulation demonstrates that resonance control can be utilized to decelerate a ballistic reentry vehicle from high hypersonic velocity at relatively low altitude to subsonic velocity prior to impact. The vehicle is ultimately driven into a flat spin with enormous drag deceleration, while limiting the normal loads during angle-of-attack buildup to a prescribed value.

REFERENCES

1. Glover, L. S., "Effects on Roll Rate of Mass and Aerodynamic Asymmetries for Ballistic Reentry Bodies," Journal of Spacecraft and Rockets, Vol. 2, March-April 1965, pp. 220-225.

2. Pettus, J. J., "Persistent Reentry Vehicle Roll Resonance," AIAA Paper 66-49, January 1966.

3. Platus, D. H., "A Simple Analysis of Reentry Vehicle Roll Resonance," Air Force Space System Division, SSD-TR-67-25, El Segundo, Calif., January 1967.

4. Platus, D. H., "A Note on Reentry Vehicle Roll Resonance, AIAA Journal, Vol. 5, July 1967, pp. 1348-1350.

5. Platus, D. H., "Angle-of-Attack Control of Drag for Slender Reentry Vehicle Recovery," Journal of Spacecraft and Rockets, Vol. 13, May 1976, pp. 275-281

6. Platus, D. H., "Angle-of-Attack Control of Spinning Missiles," Journal of Spacecraft and Rockets, Vol. 12, April 1975, pp. 228-234.

7. Truitt, R. W., Hypersonic Aerodynamics, The Ronald Press Co., New York, 1959.

8. Schiff, L. B., and Tobak, M., "Results from a New Wind-Tunnel Apparatus for Studying Coning and Spinning Motions of Bodies of Revolution," AIAA Journal, Vol. 8, November 1970, pp. 1953-1957.

9. Levy, L. L. and Tobak, M., "Nonlinear Aerodynamics of Bodies of Revolution in Free Flight," AIAA Journal, Vol. 8, December 1970, pp. 2168-2171.

GLOSSARY

A_N	normal acceleration
A_{N_c}	normal acceleration command
a,b,c	roots of Eq. (15)
c	radial c.g. offset
C_A	axial force coefficient
C_D	drag coefficient
C_L	lift coefficient
C_{m_q}	pitch damping derivative
$C^*_{m_q}$	$-C_{m_q} qSd^2/2Iu$
C_N	normal force coefficient
C_{N_α}	normal force derivative
$C^*_{N_\alpha}$	$C_{N_\alpha} qS/mu$
d	aerodynamic reference (base) diameter
g	acceleration due to gravity
h	altitude
h_0	altitude at recovery initiation
I	pitch or yaw moment of inertia
I_x	roll moment of inertia
K	feedback gain, $\omega\tau K_2/2$
K_1, K_2, K_3	feedback gains
m	vehicle mass
p	roll rate
p_o	roll rate at recovery initiation
q	dynamic pressure

R_E	earth radius
s	Laplace transform variable
S	aerodynamic reference (base) area
t	time
u	velocity
u_0	velocity at recovery initiation
x_{st}	static margin
β	$\sin^{-1} \lambda$
γ	path angle
γ_o	path angle at recovery initiation
ε	roll angle, $\pi/2 - \phi$
η	$C_{N_\alpha} qS/I_x$
η_1	$C_N(\theta)qS/I_x$
θ	angle of attack
θ_c	command value of angle of attack
$\dot{\theta}$	pitch rate in wind coordinates
λ	$\tan \sigma/\tan \theta$
μ	I_x/I
ν	pitch or yaw damping parameter, $C^*_{m_q} + C^*_{N_\alpha}$
ρ	atmospheric density
σ	cone half angle
τ	trim angle of attack asymmetry
ϕ	roll angle relative to wind
ϕ_o	meridian angle between trim asymmetry and c.g. offset (Fig. 1)
ψ	precession angle
$\dot{\psi}$	precession rate
ω	undamped natural pitch frequency
Ω	controller frequency, $(\eta\theta c)^{1/2}$

LABORATORY OPERATIONS

The Laboratory Operations of The Aerospace Corporation is conducting experimental and theoretical investigations necessary for the evaluation and application of scientific advances to new military concepts and systems. Versatility and flexibility have been developed to a high degree by the laboratory personnel in dealing with the many problems encountered in the Nation's rapidly developing space systems. Expertise in the latest scientific developments is vital to the accomplishment of tasks related to these problems. The laboratories that contribute to this research are:

Aerophysics Laboratory: Aerodynamics; fluid dynamics; plasmadynamics; chemical kinetics; engineering mechanics; flight dynamics; heat transfer; high-power gas lasers, continuous and pulsed, IR, visible, UV; laser physics; laser resonator optics; laser effects and countermeasures.

Chemistry and Physics Laboratory: Atmospheric reactions and optical backgrounds; radiative transfer and atmospheric transmission; thermal and state-specific reaction rates in rocket plumes; chemical thermodynamics and propulsion chemistry; laser isotope separation; chemistry and physics of particles; space environmental and contamination effects on spacecraft materials; lubrication; surface chemistry of insulators and conductors; cathode materials; sensor materials and sensor optics; applied laser spectroscopy; atomic frequency standards; pollution and toxic materials monitoring.

Electronics Research Laboratory: Electromagnetic theory and propagation phenomena; microwave and semiconductor devices and integrated circuits; quantum electronics, lasers, and electro-optics; communication sciences, applied electronics, superconducting and electronic device physics; millimeter-wave and far-infrared technology.

Materials Sciences Laboratory: Development of new materials; composite materials; graphite and ceramics; polymeric materials; weapons effects and hardened materials; materials for electronic devices; dimensionally stable materials; chemical and structural analyses; stress corrosion; fatigue of metals.

Space Sciences Laboratory: Atmospheric and ionospheric physics, radiation from the atmosphere, density and composition of the atmosphere, aurorae and airglow; magnetospheric physics, cosmic rays, generation and propagation of plasma waves in the magnetosphere; solar physics, x-ray astronomy; the effects of nuclear explosions, magnetic storms, and solar activity on the earth's atmosphere, ionosphere, and magnetosphere; the effects of optical, electromagnetic, and particulate radiations in space on space systems.